

International Center for Numerical Methods in Engineering

CIMNE[®]

1 9 8 7 - 2 0 1 7

30 years

generating
knowledge and solutions

Hydrodynamic analysis of a Semisubmersible Floating Wind Turbine. Numerical validation of a second order coupled analysis

SCIPEDIA

J.E. Gutiérrez-Romero^a, B. Serván-Camas^b

J.E. Gutiérrez-Romero, B. Serván-Camas,

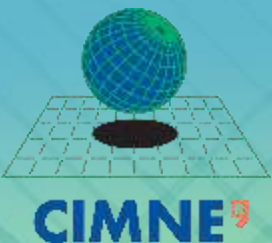
J. García Espinosa^{b,c}

Register for free at <https://www.scipedia.com> to download the version without the watermark

^a *Universidad Politécnica de Cartagena*

^b *Centre Internacional de Mètodes Numèrics en Enginyeria (CIMNE), Division of Naval
Research, Gran Capitan s/n, 08034 Barcelona, Spain*

^c *Universitat Politècnica de Catalunya, BarcelonaTech (UPC), Campus Nàutica, Edif. NT3, C.
Escar 6-8, 08039 Barcelona, Spain*



VII International Conference on Computational
Methods in Marine Engineering
Nantes, France 15–17 May 2017

OUTLINE

SCIPEDIA

✓ Introduction

✓ Hydrodynamics governing equations

✓ Numerical model

✓ Mooring models

✓ Coupling Seakeeping and Mooring

✓ Validation

Register for free at <https://www.scipedia.com> to download the version without the watermark

✓ HiPRWind model description

✓ Experimental setup

✓ Numerical setup

✓ Model calibration

✓ Analysis on bichromatic waves

✓ Analysis on irregular waves

✓ Summary and Conclusions

✓ Acknowledgements



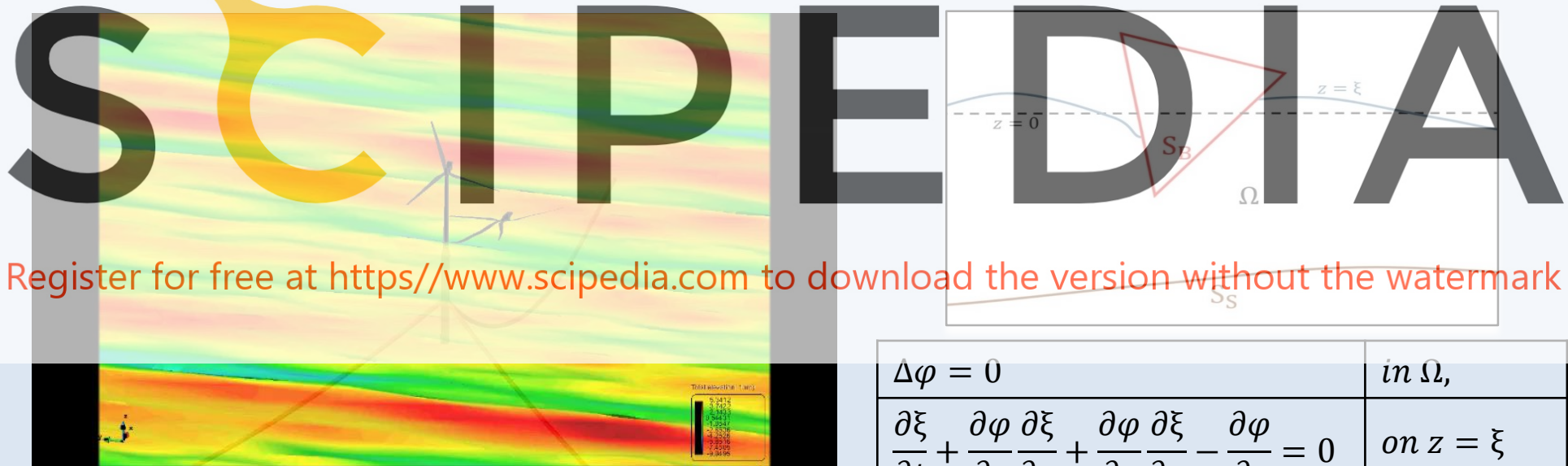
SCIPEDIA

INTRODUCTION

Register for free at <https://www.scipedia.com> to download the version without the watermark

HYDRODYNAMICS GOVERNING EQUATIONS

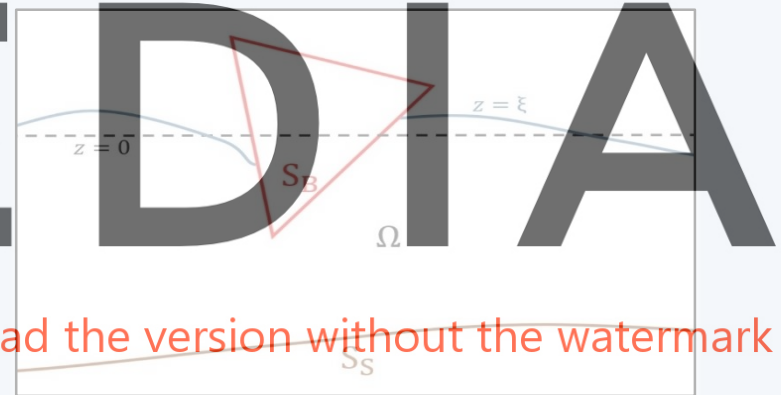
✓ Governing equations based on incompressible and irrotational flow



Register for free at <https://www.scipedia.com> to download the version without the watermark

φ : velocity potential $\mathbf{v}_\varphi = \nabla\varphi$

ξ : Free Surface elevation



| | |
|---|-----------------------|
| $\Delta\varphi = 0$ | <i>in</i> Ω , |
| $\frac{\partial\xi}{\partial t} + \frac{\partial\varphi}{\partial x}\frac{\partial\xi}{\partial x} + \frac{\partial\varphi}{\partial y}\frac{\partial\xi}{\partial y} - \frac{\partial\varphi}{\partial z} = 0$ | <i>on</i> $z = \xi$ |
| $\frac{\partial\varphi}{\partial t} + \frac{1}{2}\nabla\varphi \cdot \nabla\varphi + \frac{P_{fs}}{\rho} + g\xi = 0$ | <i>on</i> $z = \xi$ |
| $\mathbf{v}_p \cdot \mathbf{n}_p + \mathbf{v}_\varphi \cdot \mathbf{n}_p = 0$ | <i>on</i> $P \in S_B$ |
| $P_p = -\rho\frac{\partial\varphi}{\partial t} - \frac{1}{2}\rho\nabla\varphi \cdot \nabla\varphi - \rho gz_p$ | |

HYDRODYNAMICS GOVERNING EQUATIONS

- ✓ Taylor series expansion carried out to free surface boundary condition around $z=0$ to approximate the condition on $z = \xi$.
- ✓ Taylor series expansion carried out to body boundary condition around S_B^0 to approximate the condition on S_B .
- ✓ Perturbed solution:

Velocity potential:

$$\varphi = \epsilon^1 \varphi^1 + \epsilon^2 \varphi^2 + \epsilon^3 \varphi^3 + \dots$$

Free surface elevation:

$$\xi = \epsilon^1 \xi^1 + \epsilon^2 \xi^2 + \epsilon^3 \xi^3 + \dots$$

Body position:

$$\mathbf{X} = \epsilon^1 \mathbf{X}^1 + \epsilon^2 \mathbf{X}^2 + \epsilon^3 \mathbf{X}^3 \dots$$

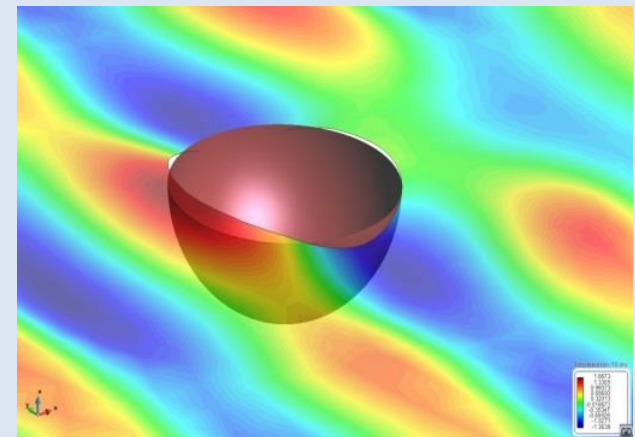
Body velocity:

$$\mathbf{V} = \epsilon^1 \mathbf{V}^1 + \epsilon^2 \mathbf{V}^2 + \epsilon^3 \mathbf{V}^3 \dots$$

- ✓ Decomposition solution: total = incident + diff-rad

$$\varphi^i = \psi^i + \phi^i; \xi^i = \zeta^i + \eta^i$$

Register for free at <https://www.scipedia.com> to download the version without the watermark



HYDRODYNAMICS GOVERNING EQUATIONS

✓ Up to second-order wave diffraction-radiation problem

✓ Governing equations (summing up first and second order equations):

| | |
|---|------------------|
| $\Delta \phi^{1+2} = 0$ | in Ω , |
| $\frac{\partial \eta^{1+2}}{\partial t} - \frac{\partial \phi^{1+2}}{\partial z} = -S^1$ | on $z=0$, |
| $\frac{\partial \phi^{1+2}}{\partial t} + \frac{r_{fs}}{\rho} + g\eta^{1+2} = -R^1$ | on $z=0$, |
| $v_{\phi}^{1+2} \cdot n_p^0 + v_{\phi}^1 \cdot n_p^1 = -(v_p^1 + v_{\psi}^1) \cdot n_p^1$ $- (v_p^{1+2} + v_{\psi}^{1+2} + r_p^1 \cdot (\nabla v_{\phi}^1 + \nabla v_{\psi}^1)) \cdot n_p^0$ | on $P \in S_B^0$ |
| $R^1 = \eta^1 \frac{\partial}{\partial z} \left(\frac{\partial \phi^1}{\partial t} \right) + \zeta^1 \frac{\partial}{\partial z} \left(\frac{\partial \phi^1}{\partial t} \right) + \eta^1 \frac{\partial}{\partial z} \left(\frac{\partial \psi^1}{\partial t} \right) + \frac{1}{2} \nabla \phi^1 \cdot \nabla \phi^1 + \nabla \psi^1 \cdot \nabla \phi^1$ | |
| $S^1 = \frac{\partial \phi^1}{\partial x} \frac{\partial \eta^1}{\partial x} + \frac{\partial \phi^1}{\partial y} \frac{\partial \eta^1}{\partial y} + \frac{\partial \phi^1}{\partial x} \frac{\partial \zeta^1}{\partial x} + \frac{\partial \phi^1}{\partial y} \frac{\partial \zeta^1}{\partial y} + \frac{\partial \psi^1}{\partial x} \frac{\partial \eta^1}{\partial x} + \frac{\partial \psi^1}{\partial y} \frac{\partial \eta^1}{\partial y}$ | |

Register for free at <https://www.scipedia.com> to download the version without the watermark

NUMERICAL MODEL

✓ Wave diffraction-radiation solver:

✓ Potential flow equation (Laplace): solved by FEM

✓ Free surface boundary condition:

✓ Combined kinematic and dynamic conditions:

$$\frac{\partial^2 \phi}{\partial t^2} + g \frac{\partial \phi}{\partial z} + \frac{\partial}{\partial t} \left(\frac{P_{fs}}{\rho} \right) + \{Q^1\} = 0$$

Register for free at <https://www.scipedia.com> to download the version without the watermark

$$\frac{\phi^{n+1} - 2\phi^n + \phi^{n-1}}{\Delta t^2} = -g\phi_z^n - \frac{1}{12}g(\phi_z^{n+1} + 10\phi_z^n + \phi_z^{n-1})$$

$$- \frac{p_{fs}^{n+1} - p_{fs}^{n-1}}{\rho 2\Delta t} - \left\{ \frac{1}{12}((Q^1)^{n+1} + 10(Q^1)^n + (Q^1)^{n-1}) \right\}$$

✓ Absorption condition: $P_{fs}(x, t) = \kappa(x)\rho \frac{\partial \phi}{\partial z}$

✓ Radiation condition: $(\phi_n^R)^{n+1} = -\frac{\phi^{n-1} - \phi^n}{c\Delta t}$

✓ Body dynamics solver

$$\bar{\mathbf{M}} \mathbf{X}_{tt} + \bar{\mathbf{K}} \mathbf{X} = \mathbf{F}$$

Temporal integrator: Newmark's scheme

MOORING MODELS

✓ Elastic catenary: quasistatic model including stiffness

✓ Reference: Jonkman, J.M. *Dynamic modelling and loads analysis of an offshore floating wind turbine*, Technical report NREL/TP-500-41958; November 2007

✓ Dynamic cable

✓ Mathematical model:

Register for free at <https://www.scipedia.com> to download the version without the watermark

✓ Cable with negligible bending and torsional stiffness.

$$(\rho_w C_m A_0 + \rho_0) \frac{\partial^2 r_l}{\partial t^2} = \frac{\partial}{\partial l} \left(EA_0 + \frac{e}{e+1} \frac{\partial r_l}{\partial l} \right) + f(t)(1+e)$$

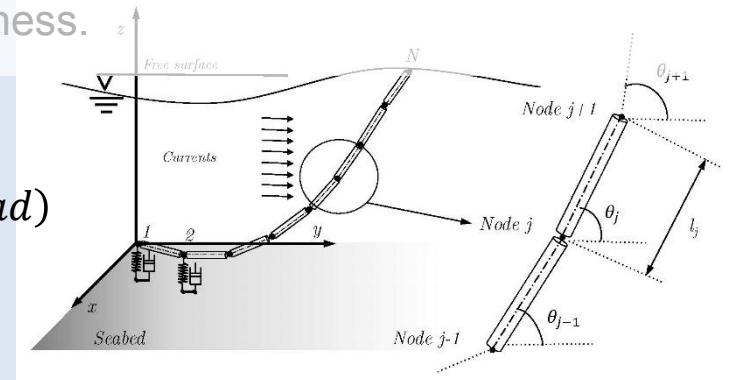
$$\frac{\partial^2 r_l}{\partial t^2} = 0, \text{ at } l = 0(\text{anchor}), \frac{\partial^2 r_l}{\partial t^2} = \ddot{r}_b, \text{ at } l = L(\text{fairlead})$$

✓ Numerical model:

✓ Solved using FEM:

✓ Includes Morison Forces

✓ Reference: Gutiérrez-Romero, J.E., Serván-Camas, B., García-Espinosa, J. and Zamora-Parra, B. *Non-linear dynamic analysis of the response of moored floating structures*. *Marine Structures* 2016; 49:116-137.



COUPLING SEEKING AND MOORING

✓ Embedded loops algorithm

✓ Three loops:

✓ Time loop

✓ Solver loop

Solve diffraction-radiation.

✓ Body dynamics loop

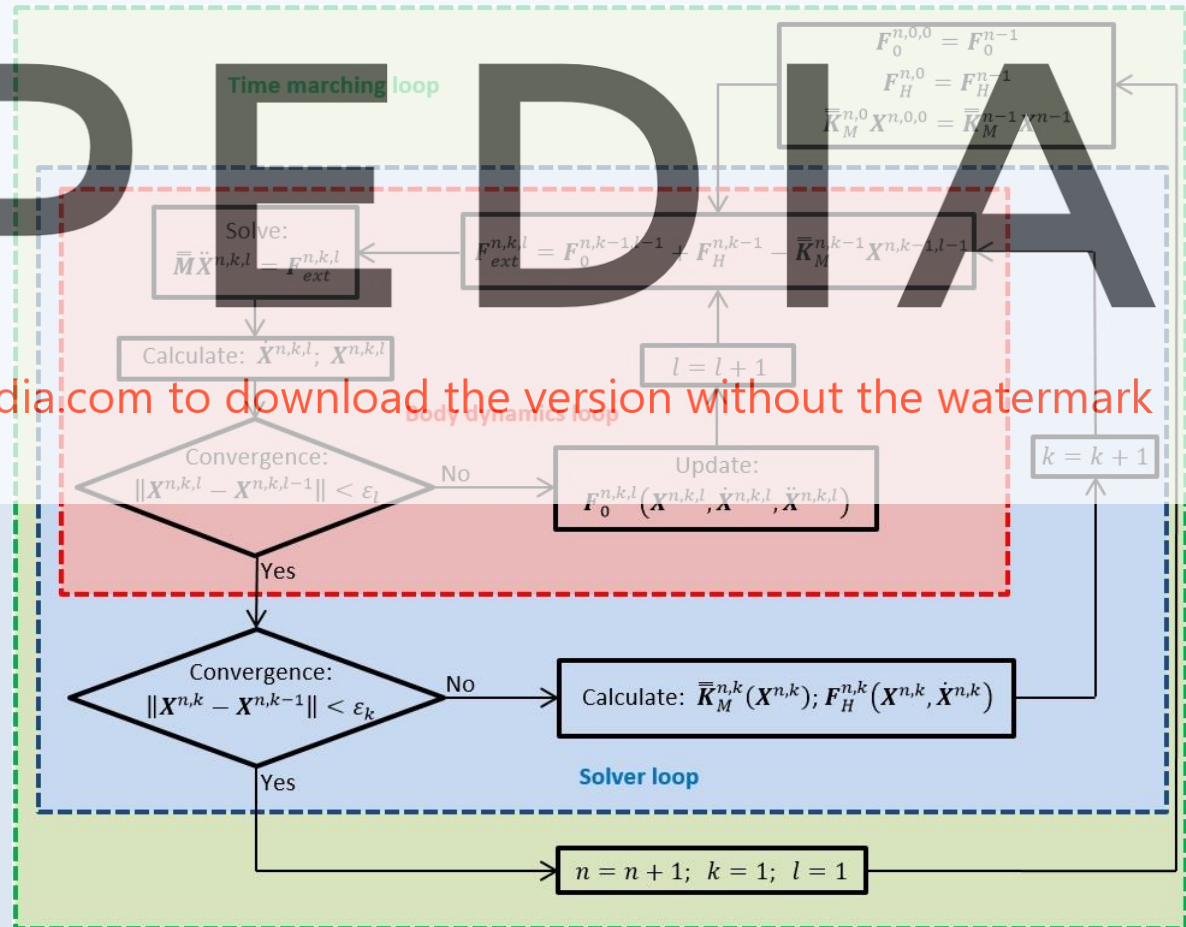
✓ Solve body movements

✓ Mooring solver:

✓ Non-linear

✓ Jacobian matrix is updated within the Solver loop

✓ Linear within the body dynamics loop.



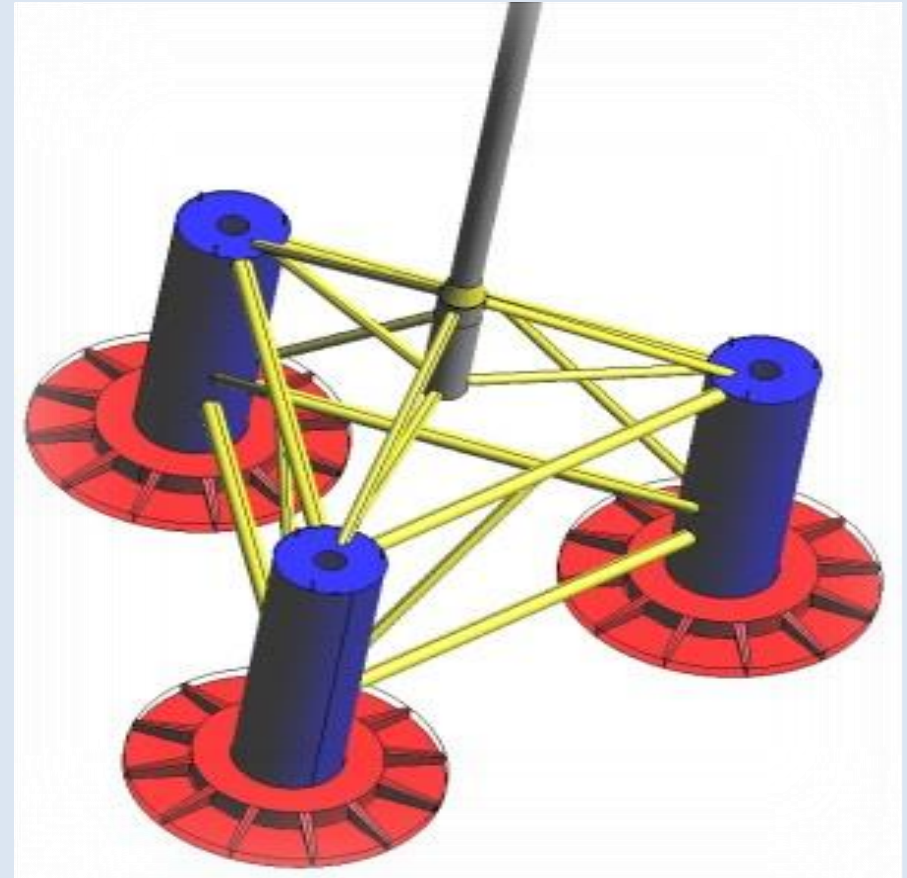
Register for free at <https://www.scipedia.com> to download the version without the watermark

VALIDATION

HIPRWIND MODEL DESCRIPTION

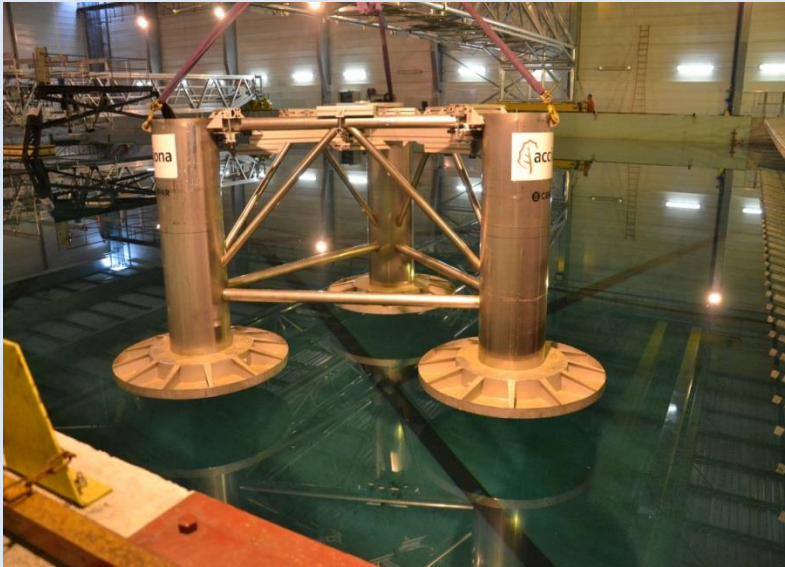
✓ HiPRWind main particulars:

| | |
|---|---------|
| Depth | 100 m |
| Operation design draft | 15.5 m |
| Distance from column center to platform center | 35 m |
| Column diameter | 7 m |
| Heave plates diameter | 20 m |
| Mass | 2332 T |
| XG | 0 m |
| YG | 0 m |
| ZG | -4.46 m |
| Radii (pitch) | 22.38 m |



EXPERIMENTAL SETUP

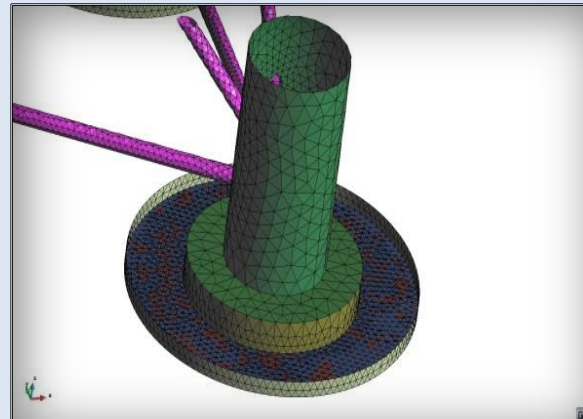
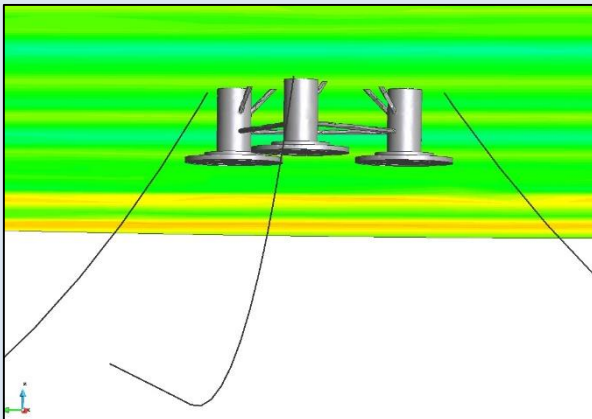
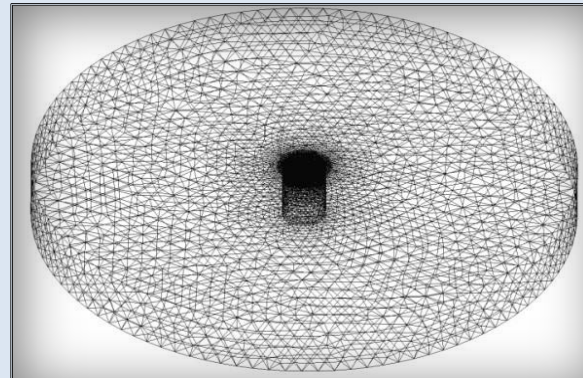
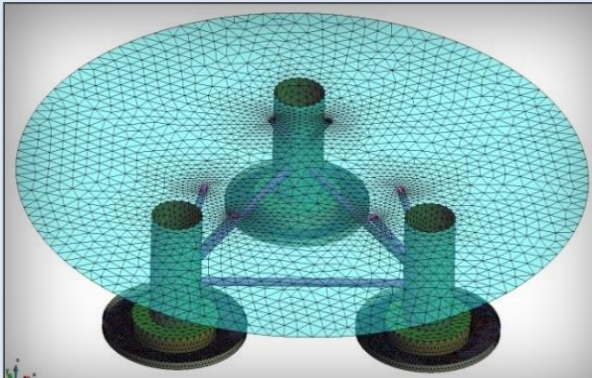
✓ Facility particulars



| Facility (model basin) | Ecole centrale de Nantes | Full scale |
|---------------------------------------|-------------------------------|------------------------|
| Model scale | 19.8 | - |
| Distance from wave generator to model | 15.10 m | - |
| Distance from beach to model | 29.45 m | - |
| Wave range | 1.35s-4.5 s (2.84m-26.34m) | 6s-20 s (56.3m520m) |
| Mooring line stiffness | 51 N/m | 20 KN/m |
| Mooring line pretension | 70.85 N | 550 KN |

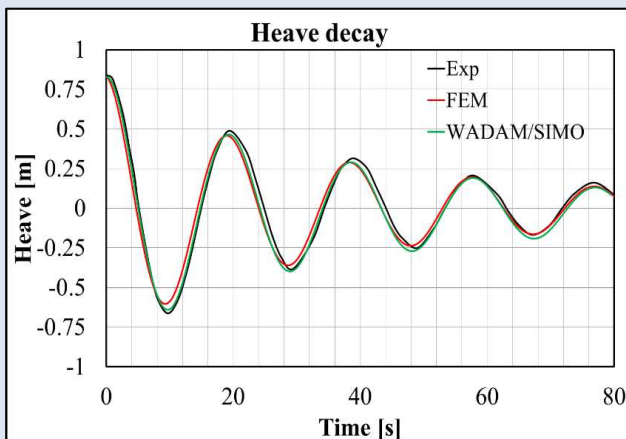
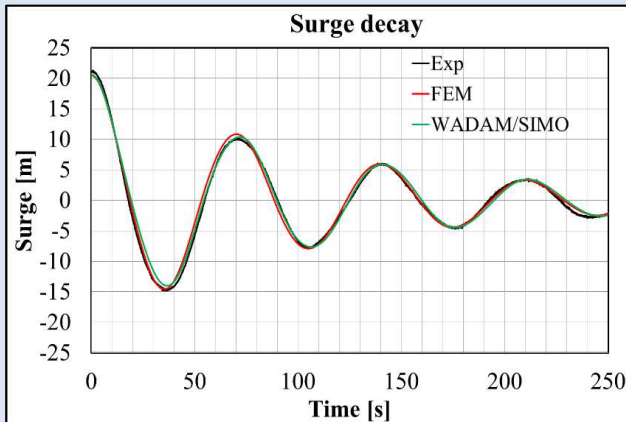
NUMERICAL SETUP

- ✓ Model geometry and mesh:
 - ✓ *Number of tetrahedral elements: 567363*
 - ✓ *Number of triangular elements: 51398*

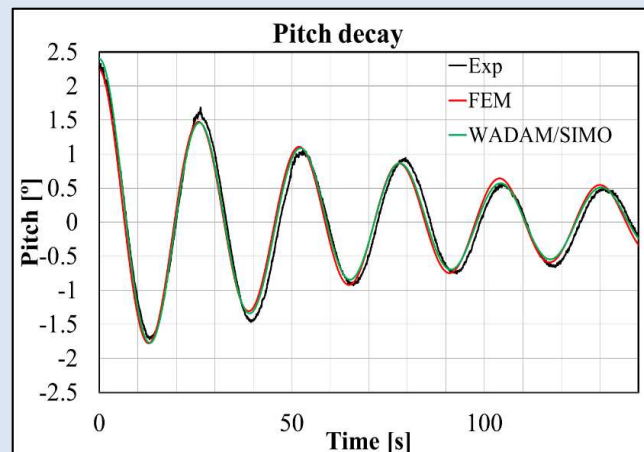


MODEL CALIBRATION

✓ Decay tests using elastic lines:



| | | FEM | WADAM/SIMO |
|--|--|------|------------|
| Applied at CG | Surge linear damping: B_{11} [KN/(m/s)] | 75 | 70 |
| | Heave added mass: A_{33} [t] | 1200 | 1000 |
| | Heave linear damping: B_{33} [KN/(m/s)] | 1100 | 110 |
| Applied at the center of each heave plate base | Heave linear damping: B_{33} [KN/(m/s)] | 76 | 50 |
| | Heave quadratic damping: B_{33}^2 [KN/(m/s) ²] | 805 | 600 |



| Natural periods | | |
|-----------------|-------|-------|
| Surge | Heave | Pitch |
| 70s | 19s | 26s |

ANALYSIS ON BICHROMATIC WAVES

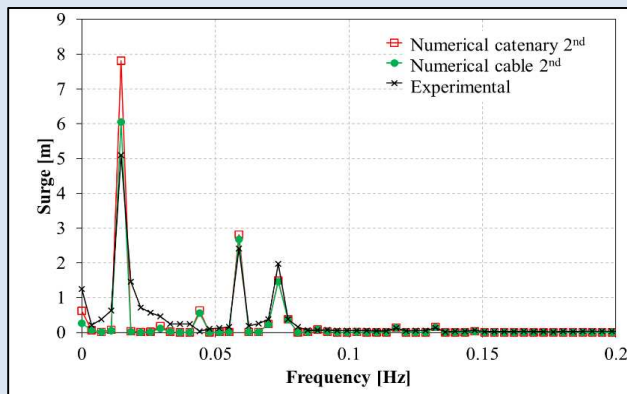
✓ Bichromatic test matrix

| Case | Incident wave 1 | | Incident wave 2 | | Freq. difference | | Freq. Sum | |
|------|-----------------|------------|-----------------|------------|------------------|----------------|------------------|---------------|
| | H_1 [m] | f_1 [Hz] | H_2 [m] | f_2 [Hz] | $f_2 - f_1$ [Hz] | T_{diff} [s] | $f_1 + f_2$ [Hz] | T_{sum} [s] |
| 1 | 5.63 | 0.0582 | 4.32 | 0.0735 | 0.0153 | 65.4 | 0.1318 | 7.59 |
| 2 | 5.27 | 0.0667 | 3.54 | 0.0813 | 0.0146 | 68.3 | 0.1480 | 6.76 |
| 3 | 2.80 | 0.1053 | 1.62 | 0.1220 | 0.0167 | 59.9 | 0.2272 | 4.40 |
| 4 | 2.13 | 0.1205 | 1.27 | 0.1351 | 0.0147 | 68.2 | 0.2556 | 3.91 |
| 5 | 1.88 | 0.1300 | 1.14 | 0.1429 | 0.0128 | 78.0 | 0.2729 | 3.66 |
| 6 | 1.50 | 0.1449 | 0.92 | 0.1587 | 0.0138 | 72.4 | 0.3037 | 3.29 |
| 7 | 1.67 | 0.1370 | 1.02 | 0.1515 | 0.0145 | 68.8 | 0.2885 | 3.47 |
| 8 | 1.35 | 0.1515 | 0.84 | 0.1667 | 0.0152 | 66.0 | 0.3182 | 3.14 |
| 9 | 1.22 | 0.1613 | 0.77 | 0.1754 | 0.0141 | 70.7 | 0.3367 | 2.97 |
| 10 | 1.11 | 0.1667 | 0.70 | 0.1818 | 0.0152 | 66.0 | 0.3485 | 2.87 |
| 11 | 2.83 | 0.0909 | 2.10 | 0.1053 | 0.0144 | 69.7 | 0.1962 | 5.10 |
| 12 | 3.37 | 0.0833 | 2.44 | 0.0997 | 0.0163 | 61.2 | 0.1830 | 5.46 |
| 13 | 4.59 | 0.0714 | 3.16 | 0.0850 | 0.0135 | 73.8 | 0.1564 | 6.39 |
| 14 | 5.64 | 0.0526 | 5.16 | 0.0672 | 0.0145 | 68.9 | 0.1198 | 8.35 |
| 15 | 2.82 | 0.0526 | 5.16 | 0.0672 | 0.0145 | 68.9 | 0.1198 | 8.35 |
| 16 | 3.44 | 0.0476 | 6.03 | 0.0625 | 0.0149 | 67.2 | 0.1101 | 9.08 |

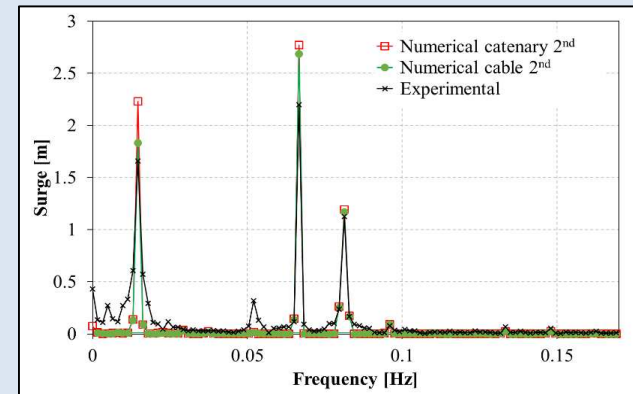
ANALYSIS ON BICHROMATIC WAVES

✓ Bichromatic test results

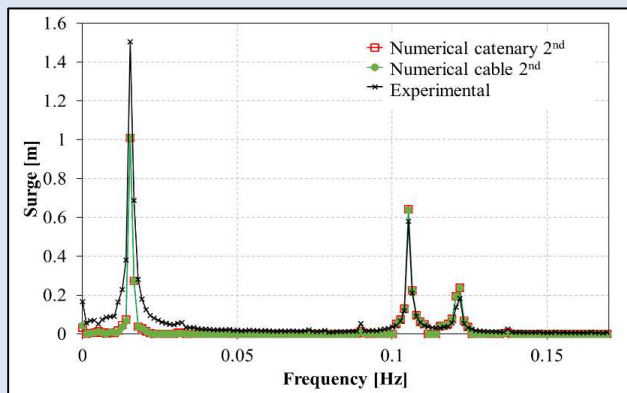
Case 1



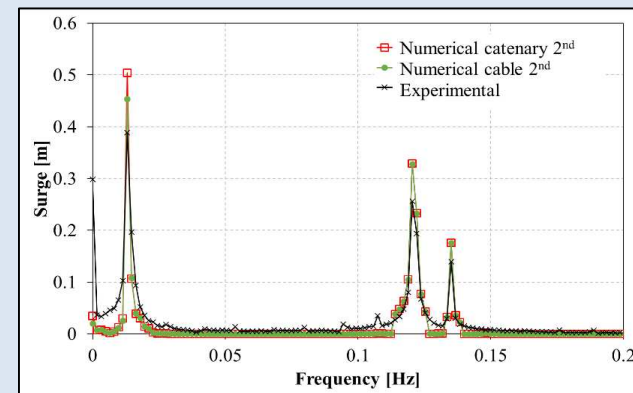
Case 2



Case 3



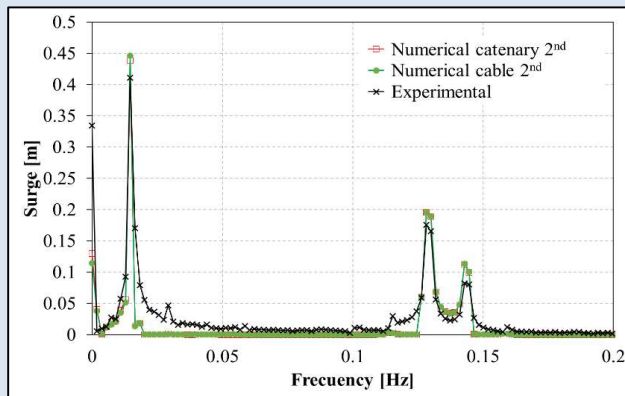
Case 4



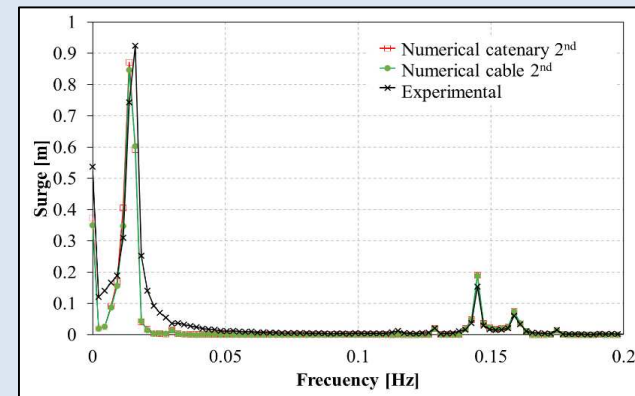
ANALYSIS ON BICHROMATIC WAVES

✓ Bichromatic test results

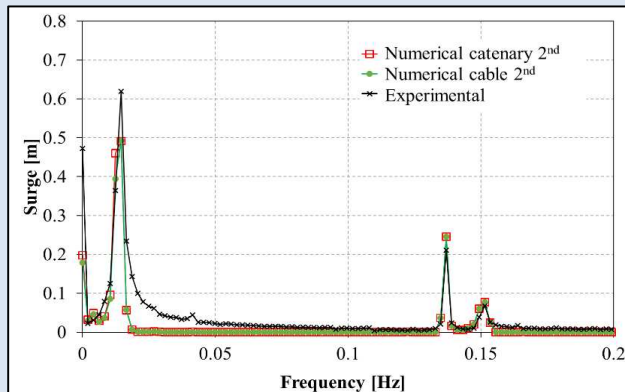
Case 5



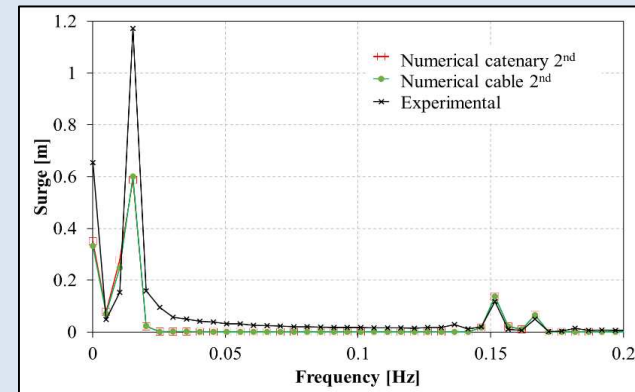
Case 6



Case 7



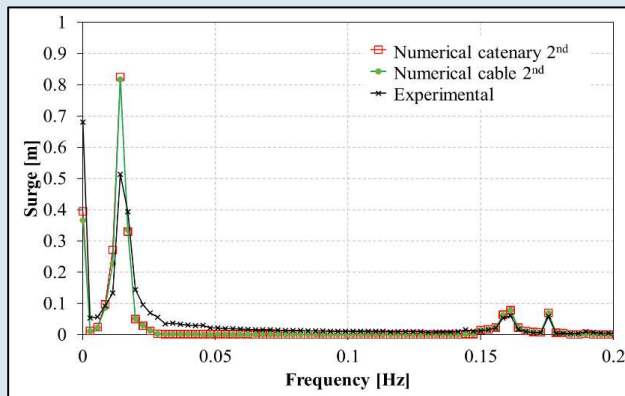
Case 8



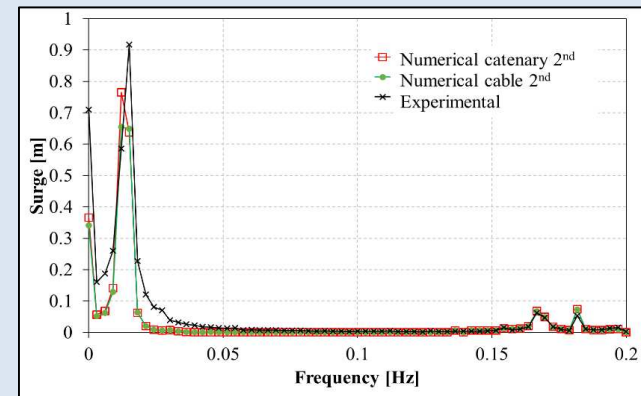
ANALYSIS ON BICHROMATIC WAVES

✓ Bichromatic test results

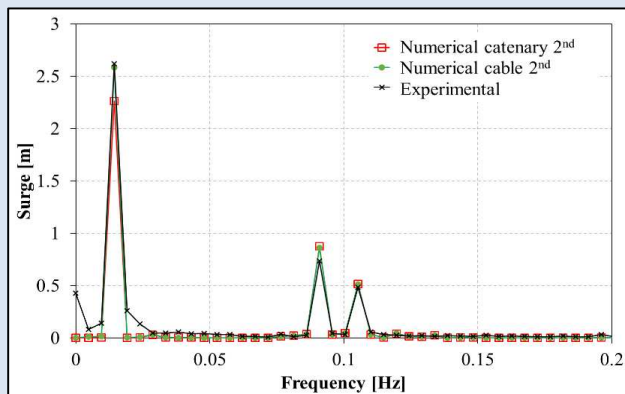
Case 9



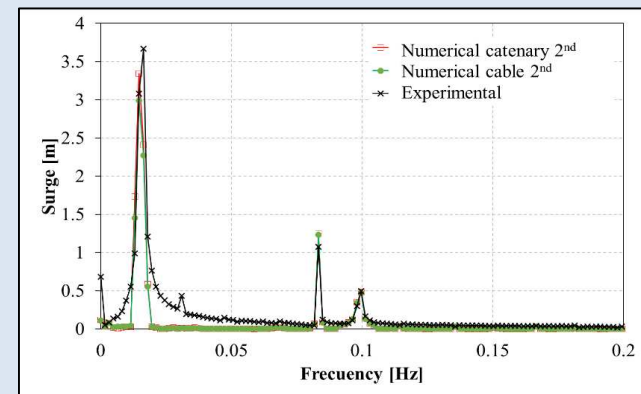
Case 10



Case 11



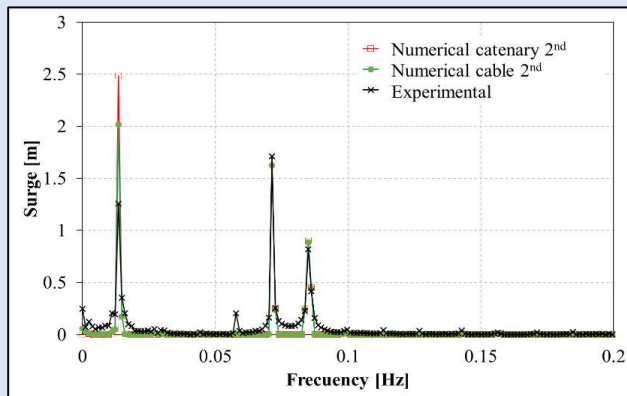
Case 12



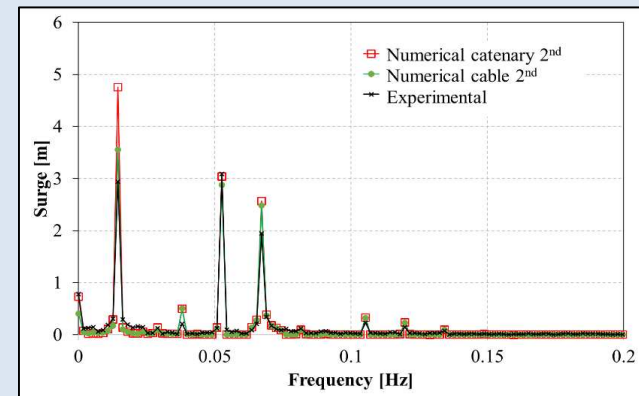
ANALYSIS ON BICHROMATIC WAVES

✓ Bichromatic test results

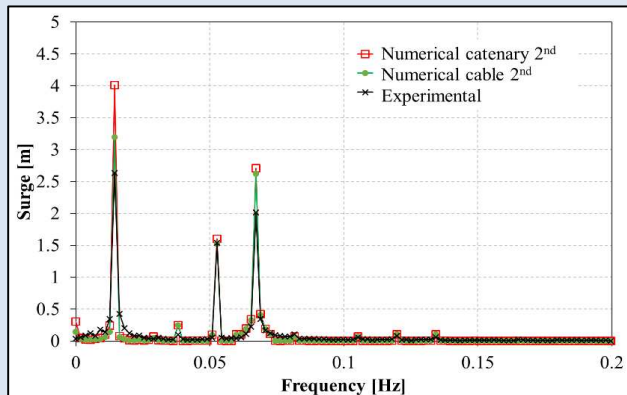
Case 13



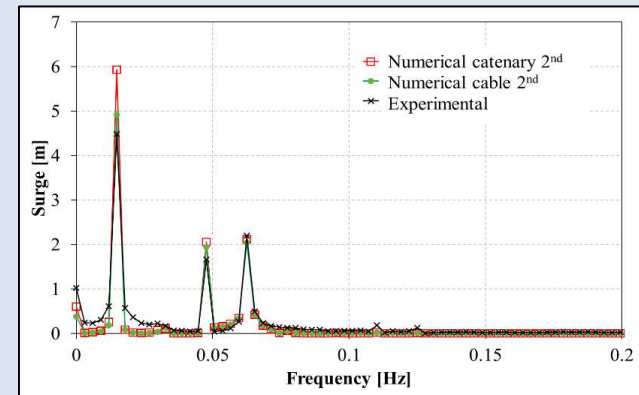
Case 14



Case 15

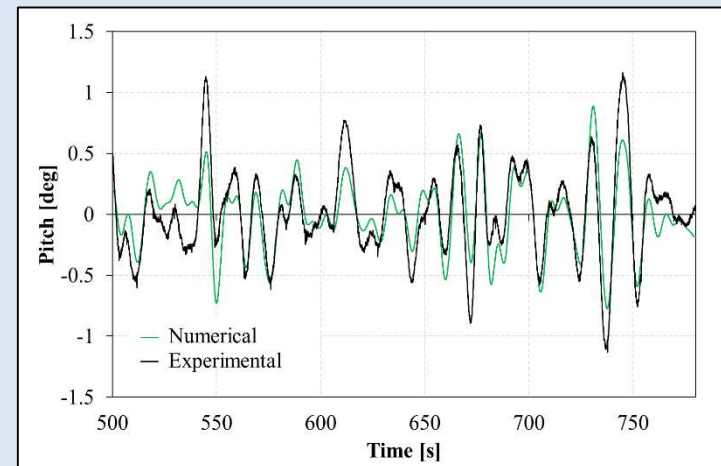
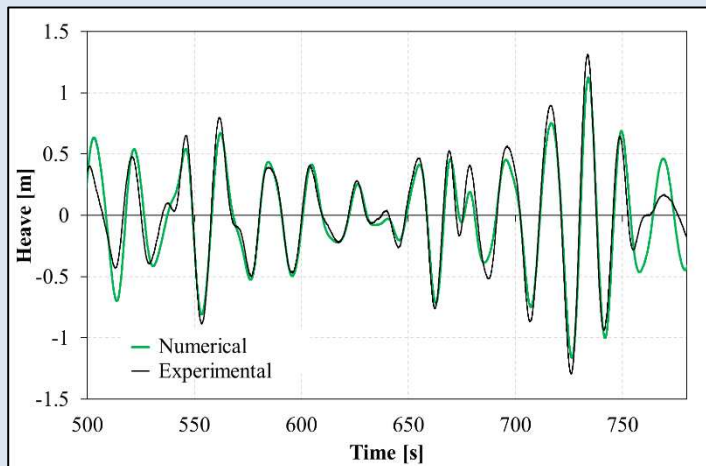
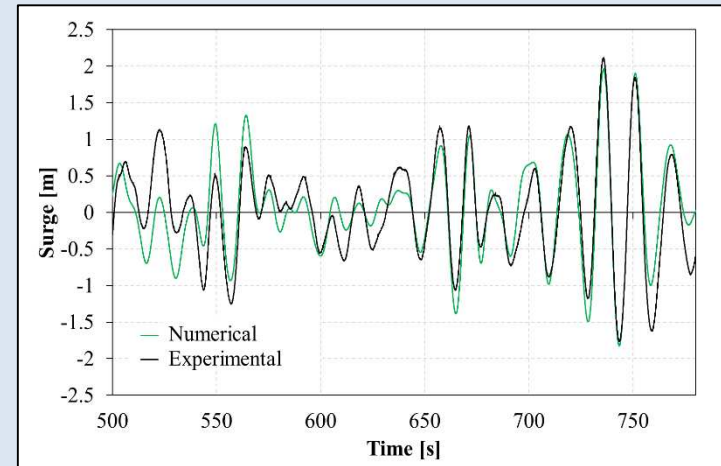
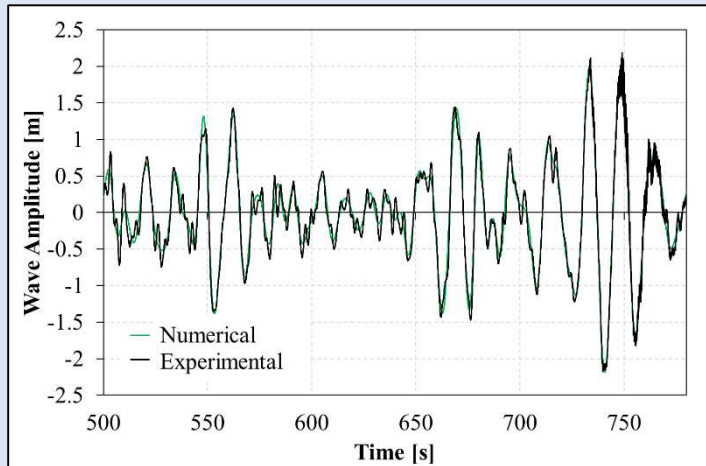


Case 16



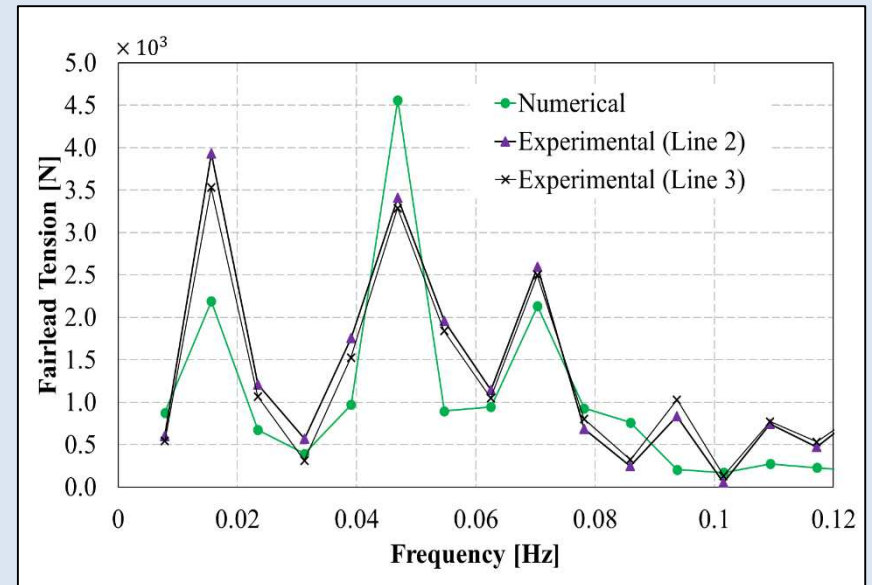
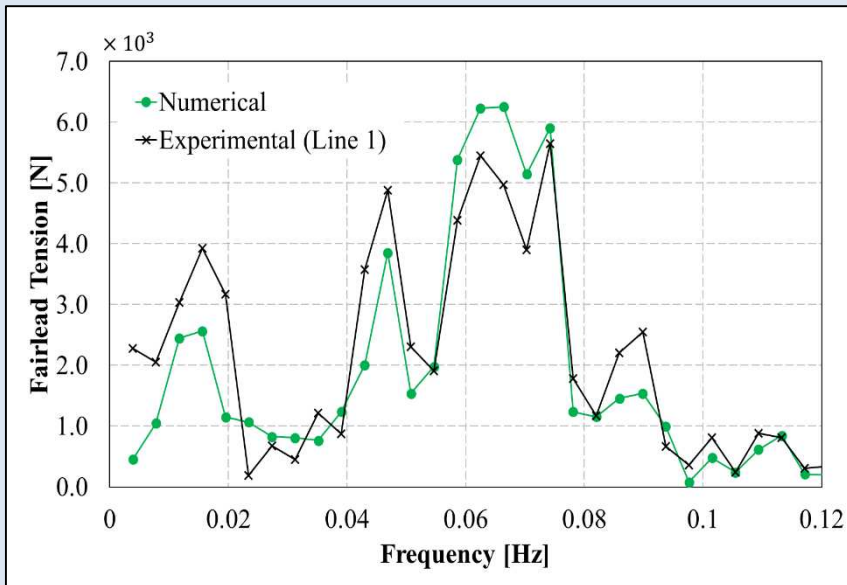
ANALYSIS ON BICHROMATIC WAVES

✓ Irregular test 1: $H_s=2.5\text{m}$, $T_p=16\text{s}$



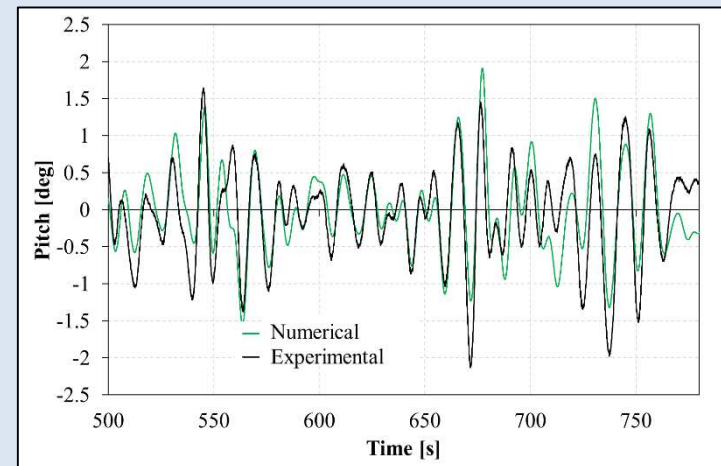
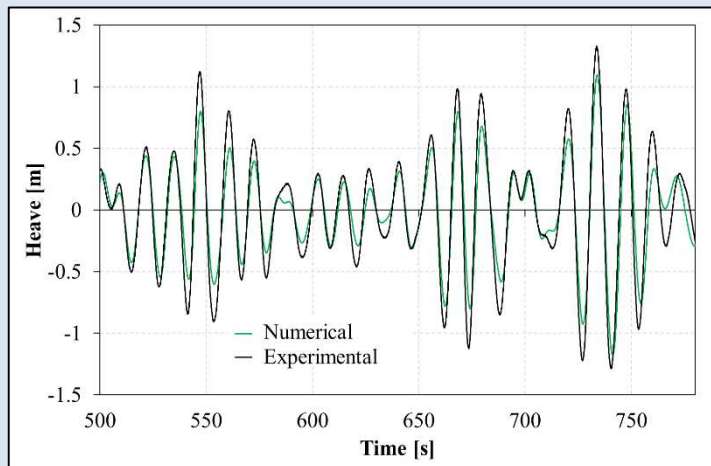
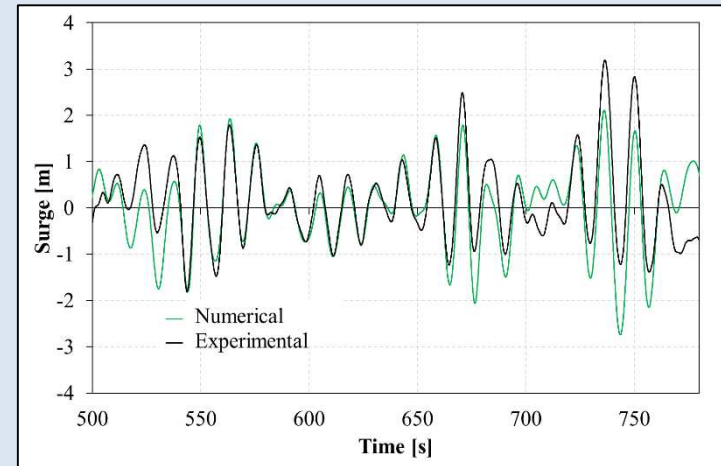
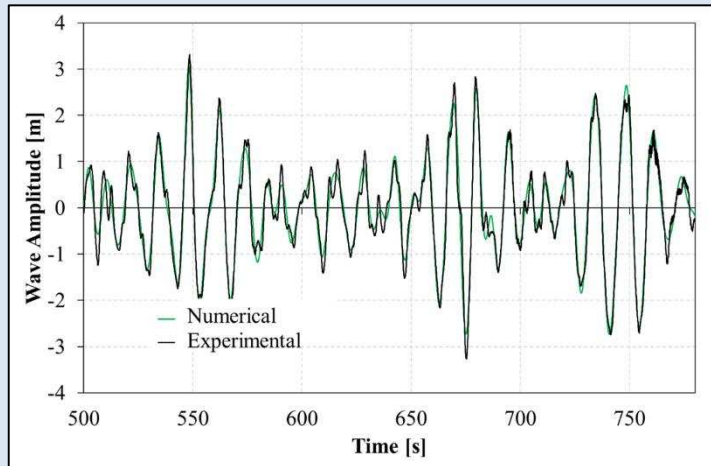
ANALYSIS ON BICHROMATIC WAVES

✓ Irregular test 1: $H_s=2.5\text{m}$, $T_p=16\text{s}$



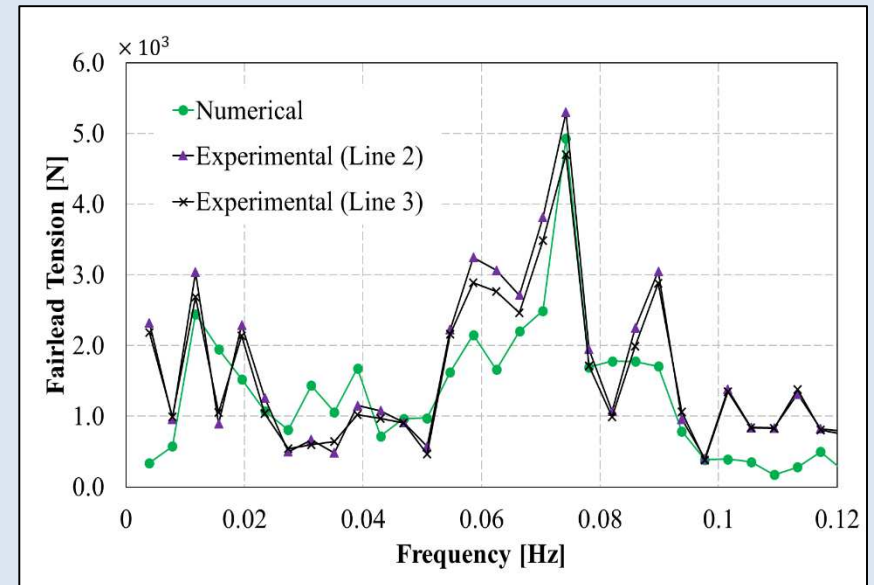
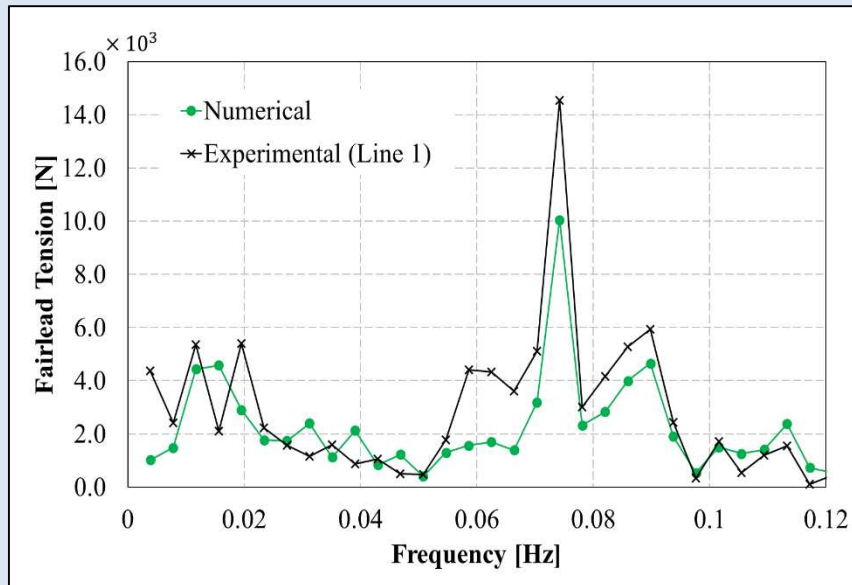
ANALYSIS ON BICHROMATIC WAVES

✓ Irregular test 2: $H_s=4.0\text{m}$, $T_p=13\text{s}$



ANALYSIS ON BICHROMATIC WAVES

✓ Irregular test 1: $H_s=4.0\text{m}$, $T_p=13\text{s}$



SUMMARY AND CONCLUSIONS

- ✓ A time-domain up to second-order wave diffraction-radiation solver based on FEM has been presented.
- ✓ Two mooring models have been coupled with the diff-rad solver.
- ✓ The proposed methodology has been validated against experiments carried out for the HiPRWind semi-submersible platform.
- ✓ Test in bichromatic waves:
 - ✓ No large differences between the elastic catenary and dynamic cable model.
 - ✓ Fair agreement between numerical and experimental (better in the higher frequency range).
- ✓ Test in bichromatic waves:
 - ✓ Good movements phase agreement.
 - ✓ Some movement deviation, mostly in the low frequency.
 - ✓ Numerical mooring loads follow the trend of the experimental measurements.

ACKNOWLEDGEMENTS

- ✓ The authors acknowledge ECN Nantes which facilities (used under the EU MARINET program) made this work possible
- ✓ The authors thank Acciona Energía and Fraunhofer Institute, and especially to Raul Manzananas, for providing the data regarding the FP7 project HiPRWind, and the “Universidad Politécnica de Madrid” for granting access to EU MARINET SEMISO project experimental results.
- ✓ Thanks to Carlos Lopez Pavon for providing the numerical results obtained with WADAM/SIMO and show in this work.
- ✓ The research leading to these results has received funding from the Spanish Ministry for Economy and Competitiveness under Grants ENE2014-59194-C2-1-R and ENE2014-59194-C2-2-R (X-SHEAKS).

International Center for Numerical Methods in Engineering

CIMNE[®]

1 9 8 7 - 2 0 1 7

30 years

generating
knowledge and solutions